

# 1 Towards a dark matter experiment

Y. Allkofer, C. Amsler, W. Creus, A. Ferella, C. Regenfus, J. Rochet, and M. Walter.

We report on our research progress on liquid argon (LAr) which is part of the DARWIN design study [1] for a next generation dark matter facility using noble liquids. More details and references to earlier work can be found in a recent publication [2]. LAr has the potential to be used as a large and sensitive target to detect nuclear recoils from Weak Interacting Massive Particles (WIMP) interactions. WIMPs would produce nuclear recoils which can be detected and isolated in noble liquids through their characteristic excitation and ionization patterns. The uncertainty in the signal calibration of nuclear recoils in LAr is large since only scarce information on the scintillation efficiency can be found in literature. In fact, the complex microscopic processes which lead to the scintillation and charge signals are not well understood at low energies.

The energy dependent light yield  $Y_{nr}$  of nuclear recoils is described by the relative scintillation efficiency  $\mathcal{L}_{\text{eff}}$  which compares the light yield of electrons to that of nuclear recoils (by convention  $\mathcal{L}_{\text{eff}}$  is measured at zero electric field). Its value is determined by the product of two quenching processes. Towards low energies, an increasing fraction of the recoil energy is lost to heat (nuclear quenching). The density of the excited or ionized states produced during the stopping process depends on their interaction (luminescence quenching). The light yield of electrons is not affected by nuclear effects and is proportional to the energy deposit above some tens of keV. The relative scintillation efficiency is expressed as  $\mathcal{L}_{\text{eff}} = E_{ee}/E_r$ , where  $E_{ee}$  stands for the energy of an electron producing the same amount of light as a recoiling nucleus with energy  $E_r$ . In contrast to xenon, a separation of the scintillation signal in fast ( $\tau_1 = 6$  ns) and slow ( $\tau_2 = 1.6$   $\mu$ s) components is possible in LAr. This effect is exploited to reduce background in LAr dark matter detectors.

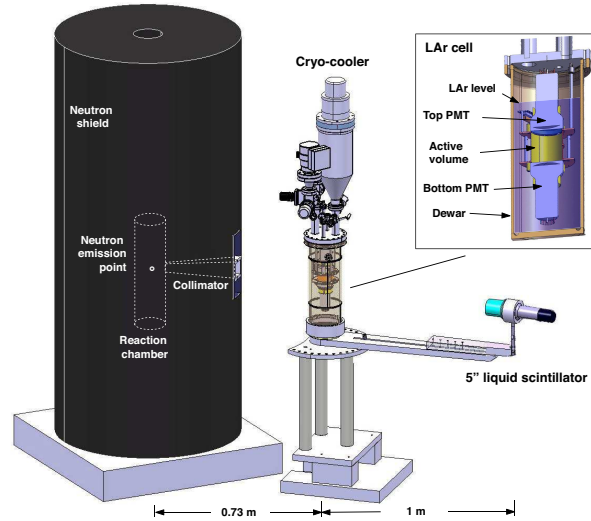


FIG. 1.1 –  $n - n - Ar$  scattering experiment with neutron generator, shield and zoom on the LAr cell.

We present an overview of the experimental method to determine  $\mathcal{L}_{\text{eff}}$  and show first results from data recorded under neutron,  $\alpha$  and  $\gamma$ -irradiation in LAr at zero electric field. The experimental setup is shown in Fig. 1.1. We induce nuclear recoils in the LAr cell by 2.45 MeV neutrons from a deuterium-fusion-generator (from NSD-Fusion, Germany). It delivers up to  $2 \times 10^6$  isotropically emitted monoenergetic neutrons from the two-body reaction  $dd \rightarrow {}^3\text{He} + n$ . The fusion rate in the deuterium plasma is controlled by an electrical DC field generated by an adjustable constant current HV supply. The environment is shielded from neutron and X-ray radiation by a 1600 kg polyester cylinder with 2 mm Pb cladding. A polyethylene collimator with square cross section restricts the emission of neutrons in a solid angle of about 0.2% of  $4\pi$ . Liquid scintillator counters (LSC) detect the scattered neutrons at various angles.

The cryogenic cell is shown in the inset. Two tetraphenyl-butadiene (TPB) coated 3" PMTs (Hama-

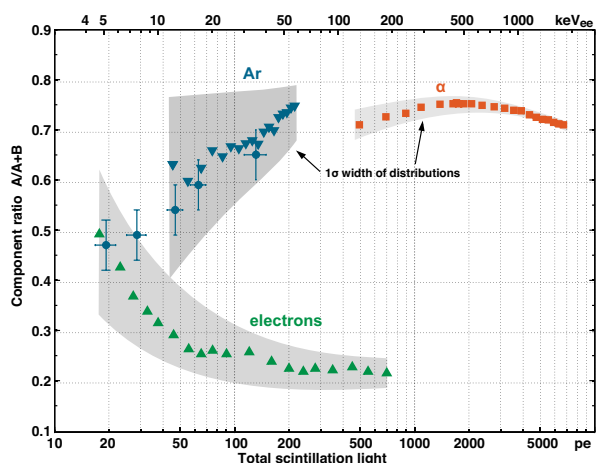


FIG. 1.2 –  $CR$  vs. light yield for Ar-,  $\alpha$ -recoils and electrons. The grey zones indicate the  $1\sigma$  spread.

matsu R6091-MOD) with bialkali photo cathodes and Pt underlay ( $QE \approx 15\%$ ) are arranged face to face, forming a cylindrical sensitive volume of roughly  $0.2 \ell$ . The cell walls are covered with a TPB coated reflector foil [3, 4] to shift the VUV scintillation light (128 nm) to  $\sim 420$  nm. A  $^{210}\text{Po}$   $\alpha$ -source is installed in the center of the cell. A turbopump is used to evacuate the chamber to typically  $10^{-6}$  mbar prior to filling with argon gas class 60. A membrane pump provides for recirculation via OXISORB cartridges which reduce the  $\text{O}_2$  and  $\text{H}_2\text{O}$  contamination. The gas is condensed on top of the chamber by a (Sumitomo CH210) cryocooler. A LabView slow control regulates the cold head temperature and records temperatures, pressures and liquid levels.

The analogue signals from the two PMTs are each split into two inputs (for a larger dynamic range) and sampled with an oscilloscope with 5000 points at 1 GS/s. LAr signals are integrated numerically from the digitized currents of the PMTs, normalised to their mean single photon charges. Light yield calibrations were performed regularly with an external  $^{241}\text{Am}$  source producing a prominent 60 keV photopeak.

In LAr VUV fluorescence from the so-called second continuum is the dominant mechanism for light emission. The light pulse shape is described by the sum of two exponentials with amplitudes describing the radiative decays of two fundamental

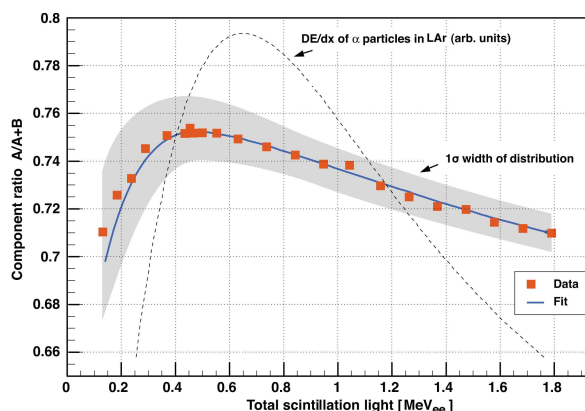


FIG. 1.3 –  $CR$  for  $\alpha$ s in LAr and fit versus total scintillation light in MeV (electron equivalent).

excimer states (singlet and triplet, with lifetimes  $\tau_1$  and  $\tau_2$ , respectively). Due to their long lifetime triplet states undergo collisions with neighbouring particles before decaying. Interactions with impurities can cause their (non-radiative) destruction, inducing losses in the slow scintillation light and a reduction in  $\tau_2$ . In the following our component ratio ( $CR$ ) – the relative strength of the fast component of the scintillation light – is corrected for this effect by extrapolation to pure LAr [2, 5].

The  $CR$ s are determined for recoiling Ar nuclei (induced by neutrons),  $\alpha$ -particles (from the  $^{210}\text{Po}$  source) and electrons (induced by 511 keV  $\gamma$ s from an external  $^{22}\text{Na}$  source). A coincidence with an external detector was required for the photon data to tag the emission of two 511 keV  $\gamma$ s. This data was also used to determine the time-of-flight calibration. Figure 1.2 shows the  $CR$  distribution versus total amount of scintillation light. The two prominent bands from electrons and nuclear recoils merge for energies below about 10 keV $_{ee}$ . The values at low energies for argon recoils are also shown (circles). There is a correlation between  $CR$  and the stopping power. Large ionisation densities lead to strong interaction between particles and produce a larger fraction of singlet states. For electrons  $CR$  is equal to  $\sim 0.25$  at the minimum ionisation densities, close to the statistical weights of 1 : 3 for the isolated production of singlet and triplet states (no interaction between them).

The relation between population of excimer states at various energy losses can be unfolded by taking

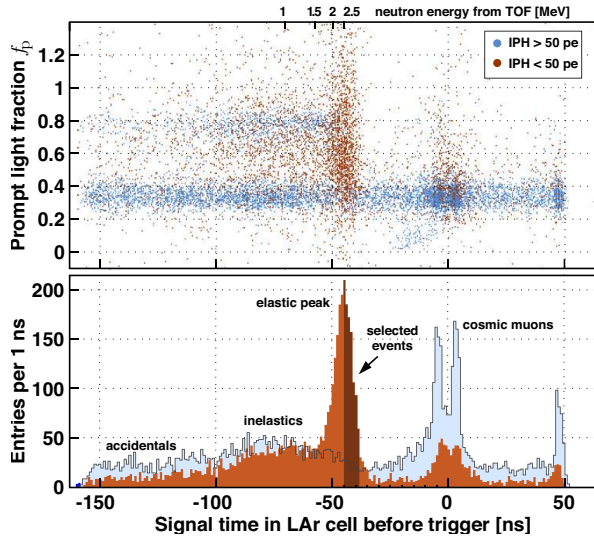


FIG. 1.4 – Prompt light fraction  $f_p$  vs. signal time in LAr and projection on the time axis for neutrons triggering the liquid scintillator counter.

into account the integral over the stopping range. We have determined the energy scale for  $\alpha$ -particles by assuming a linear relation between  $CR$  and the energy transfer [2]. A value of  $\mathcal{L}_{\text{eff}}^{\alpha} = 0.74 \pm 0.04$  was found for the mean relative scintillation efficiency for  $\alpha$ -particles in LAr in the range 0.18 – 2.5 MeV (Fig. 1.3). The light loss of  $\simeq 25\%$  is entirely due to luminescence quenching.

We now present the data taken with the neutron generator. A 5" liquid scintillator (LSC) was positioned at 30, 40, 50, 60 and 90°, at 1 m from the target, corresponding to 16, 28, 43, 60 and 120 keV recoil energies, respectively. The neutron flux (typically  $2 \times 10^5$  n/s into  $4\pi$ ) was chosen so that accidental background induced by bremsstrahlung was kept at an acceptable level. About 1 n/min scattered off an argon nucleus in the active volume and was detected in the LSC. The direct line of sight between the exit of the collimator and the LSC was obstructed by a 20 cm thick sheet of polyethylene. Background rates were around 5/min, originating mainly from cosmic muons saturating the LSC, and accidental coincidences between diffusively scattered neutrons and bremsstrahlung. Events in the LAr cell were accepted whenever both PMTs showed signals above 0.2 photoelectrons (pe) in a 50 ns time coincidence. A trigger was generated by a LAr signal within a window of [-150, +50] ns

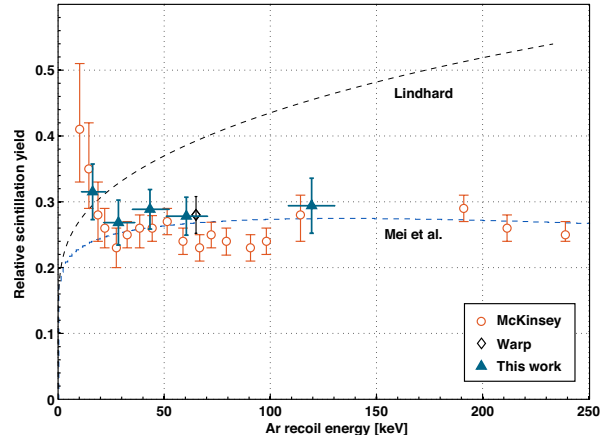


FIG. 1.5 –  $\mathcal{L}_{\text{eff}}$  from this work compared to theory and previous data.

around the arrival time of a neutron in the LSC.

Figure 1.4 shows the prompt light fraction  $f_p$  vs. the time difference between the signals in the LAr cell and the LSC for the 30° data (19k events). Here  $f_p$  is the ratio of the scintillation light yield in the first 50 ns to the total light. The time projection is shown in Fig. 1.5. The distribution of signals ( $< 50$  pe) is dominated by elastically scattered neutrons around the nominal flight time at -45 ns (brown histogram). Also visible are inelastic scatters from neutrons and a small background from accidental coincidences of diffusely scattered neutrons with bremsstrahlung in the outer LAr volume. Requiring at most 50 pe removes many of these events and also cosmic muons (blue histogram). A 5 ns wide TOF cut then selects elastic scatters ( $\sim 1'000$  events, black area). Figure 1.5 shows our measurements at the five angles, together with the data from refs. [6, 7]. Our measurements lead to the average  $\langle \mathcal{L}_{\text{eff}} \rangle = 0.29 \pm 0.03$  for nuclear recoils above 20 keV (or 6 keV electron equivalent). The data are consistent with a constant value for  $\mathcal{L}_{\text{eff}}$ , in accord with a simple saturation law combined with the Lindhard model [8].

Summarizing, we confirm that scintillation light quenching in LAr by impurities is similar to that in gaseous argon [5]. As in the latter work we use measured lifetimes and component ratios to reconstruct purity independent results. We confirm values for  $CR$  monotonically increasing with energy transfer.

A  $CR$  value of 0.25 close to the one expected from statistically populated singlet and triplet states is observed for electrons in the region of lowest ionization densities. For nuclear recoils we find  $CR$  rising from 50% to 75% between 20 and 200 keV. For  $\alpha$ -particles in the MeV range we determine a relative scintillation yield  $\mathcal{L}_{\text{eff}}^{\alpha} = 0.74 \pm 0.04$ . Within present errors our value of the relative scintillation yield  $\mathcal{L}_{\text{eff}}$  is constant for nuclear recoils at energies between 16 and 120 keV, with a mean value of  $0.29 \pm 0.03$ . A refined analysis is in progress [9].

4

No conclusive results below 16 keV can be drawn from the present analysis. We are upgrading the cell with PMTs of larger quantum efficiency and are improving the cleaning system. An internal electric field will be added to extract the ionization charge from the liquid and to determine field and energy dependences of both light and charge yields in LAr, at working points relevant to dark matter searches.

- [1] L. Baudis, arXiv:1012.4764v1 [astro-ph.IM] (2010) and <http://darwin.physik.uzh.ch/>
- [2] C. Regenfus *et al.*, arXiv:1203.0849v1 [astro-ph.IM] (2012).
- [3] V. Boccone *et al.*, J. of Instrumentation **4** (2009) P06001; V. Boccone, PhD-thesis, Universität Zürich, 2010.
- [4] M. Walter, Diploma-Thesis, Universität Konstanz, 2011.
- [5] C. Amsler *et al.*, J. of Instrumentation **3** (2008) P02001.
- [6] R. Brunetti *et al.*, New Astr. Rev. **49** (2005) 265.
- [7] D. Gastler *et al.*, arXiv:1004.0373v2 [physics.ins-det] (2011).
- [8] D. Mei *et al.*, Astropart. Phys. **30** (2008) 12.
- [9] W. Creus, PhD-Thesis, Universität Zürich (in preparation).